Dynamic Analysis of Structures with Friction Forces at Sliding Junctures

David Hunt* and William Adams†
The Aerospace Corporation, El Segundo, California
and
Tim Bock‡
MacNeal-Schwendler Corporation, Pasadena, California

This paper presents the procedure and rationale of two methods for determining the dynamic response of structures with friction forces at sliding junctures. A discrete element model of the structure is used which permits a concise matrix formulation of the problem. The primary contribution in this work is accountability for time-dependent sliding friction forces which are treated as external loads. In one method, the sticking of sliding junctures is simulated by a standard approach used for Coulomb dampers. For the other method, sticking is taken into account for the first time in a discrete element analysis. Numerical results from both methods are compared.

Nomenclature

B = modal damping, diagonal matrix
C = modal stiffness, diagonal matrix
D_n, D_{nn} = column matrices, values are discrete damper coefficients, linear and nonlinear, Eq. (8)
$\dot{d}_r$ = relative velocity of discrete dampers
E_l = selector matrix, Eq. (11)
F = diagonal matrix of coefficients of friction for all sliding-sticking junctures
k = scalar value, Eq. (8)
P_d = discrete damper forces
P_f = friction force values at all sliding-sticking junctures
P_{ff} = attachment friction forces for all sliding junctures, zero values for all sticking junctures
P_{io} = normal force components at all sliding-sticking junctures
P_{qd} = modal forces due to discrete dampers
P_{qe} = modal forces due to externally applied loads
P_{qs} = modal forces due to sliding and sticking attachment forces at all sliding-sticking junctures
P_r = resultant of normal force components at each sliding-sticking juncture
P_{ss} = $P_{ff}+P_{st}$ = attachment forces at all sliding-sticking junctures, due to sliding friction and sticking
P_{st} = attachment forces for all sticking junctures, zero values for all sliding junctures
$Q, \dot{Q}, \ddot{Q}$ = modal displacements, velocities, and accelerations
$T_{ac}, T_{df}, T_{fs}, T_{di}$ = load transformation matrices, Eq. (10)
T_n = diagonal matrix of $\dot{d}_r$ values
T_{nn} = diagonal matrix of $\dot{d}_r\,|\dot{d}_r|^k$ values
T_{rd} = modal transformation matrix, Eqs. (7) and (9)
T_{rs} = modal transformation matrix, Eqs. (4), (6), and (12)
$X_r, \dot{X}_r, \ddot{X}_r$ = relative displacements, velocities, and accelerations for all sliding-sticking junctures
X = $P_{qe}+P_{qd}-B\dot{Q}-CQ$
$\tilde{\mu}, \dot{\tilde{X}}_r$ = parameters which define coefficient of friction for the ramp method, Fig. 2
μ = coefficient of friction

Submitted May 14, 1982, revision received July 26, 1983.

*Member of Technical Staff, Vehicle Engineering Division.
†Member of Technical Staff, Information Processing Division.
‡Senior Analyst.

Introduction

CALCULATION of the dynamic response of space structures with translational and rotational sliding friction junctures has offered a long-term problem.

A typical sliding connecting juncture is a bearing and a shaft. The juncture permits a relative sliding displacement with a friction force corresponding to the sliding degree of freedom (DOF). The usual approach employed in a problem of this nature is a linear analysis accomplished by ignoring friction effects.

Because of space vehicle design considerations, such as loads, temperature, material compatibility, and weight, the coefficient of friction at such junctures can be on the order of 0.1. This is not negligible, and for these cases friction forces can be significant. An investigation of their effect is necessary.

During the dynamic response, friction effects can cause a sliding juncture to stick or lock up for a short time. The stiffness matrix of the structure is, therefore, time dependent. Based on a discrete element model, the dynamic response of a structure with a time-dependent stiffness matrix was treated in Ref. 1; however, friction effects were neglected.

Prior to this work published papers considered simplified structures in problems of this nature with mathematical solutions based on partial differential equations as opposed to numerical solutions. These published approaches go back over 100 years to the work of Willis,[2] who investigated the dynamics of a mass moving along an elastic structure.

Coulomb friction effects are taken into account in this paper. Two approaches are presented based on a discrete element model of the structure. These are termed herein as the

ramp and stuck methods. Included in both methods is a formulation accounting for nonlinear discrete dampers.

The ramp method[3] is a standard approach for Coulomb damper problems. Sticking is approximated by restricting the magnitude of the sliding friction force between pairs of sliding DOF to small values during the simulated sticking phase.

In the stuck method, sticking at sliding junctures is taken into account for the first time in a large discrete element analysis problem. A unique characteristic of the sliding-sticking juncture problem is the occurrence of discontinuities in accelerations. This is explained in the formulation for the stuck approach. There are no discontinuities in the ramp method. Here, they are approximated and smoothed out.

The ramp and stuck methods have been coded for a digital computer. To compare approaches, a specific numerical example is considered; namely, the inertial upper stage payload and the Space Shuttle launch vehicle subjected to a liftoff loading condition. Sliding-sticking junctures are at seven of the payload-launch vehicle attach nodes (one at each node) and at three internal payload nodes (two at each node) for a total of 13 pairs of sliding-sticking DOF. In this example, torsional friction effects were neglected.

The Space Shuttle has a critical load capability in the yaw direction which corresponds to the direction of several sliding friction forces. Therefore, a capability for rigorously investigating sliding friction forces is important. The methods discussed herein can apply to other payloads and launch vehicles and to sliding friction dynamic problems outside of the aerospace field.

Method of Analysis

The physical coordinates of the discrete element model are transformed to modal coordinates Q. Sliding friction and sticking forces between sliding-sticking pairs of DOF are treated as external loads as well as forces from the nonlinear discrete dampers. The matrix differential equation of motion is

$$\ddot{Q}+B\dot{Q}+CQ=P_{qe}+P_{qs}+P_{qd} \tag{1}$$

Discrete friction forces at each of the sliding-sticking junctures make up the P_f column matrix; it is computed from the Coulomb-Morin friction law expressed as

$$P_f=FP_r \tag{2}$$

The formulation of the P_r column matrix is discussed in reference to Eq. (11). As the P_r matrix forces depend on sliding friction and sticking attachment forces and discrete damper forces [see Eqs. (10) and (11)], the formulation of these latter forces is considered first.

The values of sliding friction forces with positive values and for all sliding-sticking junctures make up the P_f matrix. Each value in the P_f matrix represents the value of each force of a pair of sliding friction forces. The values of sliding friction forces in the P_f matrix include those for junctures which are in the sticking phase. These are used for comparison checks for determination of a change from sticking to the sliding phases. This point is discussed later.

In the derivation which follows, it is convenient to consider the column matrix of attachment forces for all sliding-sticking junctures, P_{ss}, as the sum of two column matrices, P_{ff} and P_{st}. Thus,

$$P_{ss}=P_{ff}+P_{st} \tag{3}$$

The nonzero values in the P_{ff} matrix are the sliding friction forces corresponding to junctures which are sliding. These values are from the P_f matrix, but with the same sign as the juncture relative velocity. For sticking junctures the corresponding values in the P_{ff} matrix are zero. The relative displacement and velocity vectors, X_r and $\dot{X}_r$, for each pair of sliding-sticking DOF are computed from

$$X_r=T_{rs}Q, \qquad \dot{X}_r=T_{rs}\dot{Q} \tag{4}$$

A positive value in the P_{ff} matrix is taken as representing a pair of physical sliding friction forces which result from a positive change in relative displacement (which is due to a positive relative velocity). This positive physical force direction can be determined from juncture kinematics.

The nonzero values in the P_{st} matrix are values of attachment forces for all sticking junctures. For sliding junctures, the corresponding values in the P_{st} matrix are zero. Computation of the P_{st} matrix is discussed in the Stuck Method section. A positive value in the P_{st} and P_{ss} matrices represents a pair of physical forces at a juncture in the same direction as the positive physical sliding friction forces.

To explain the formation of the P_f, P_{ff}, P_{st}, and P_{ss} matrices, a structure is considered with only two sliding-sticking junctures. Figure 1 shows these sliding-sticking junctures with clearances between contacting surfaces exaggerated for clarity.

Normal forces at each juncture are P_{r1} and P_{r2}. From Eq. (2), the P_f matrix is

$$P_f=\begin{Bmatrix} P_{f1} \\ P_{f2} \end{Bmatrix}=\begin{bmatrix} \mu_1 & \\ & \mu_2 \end{bmatrix}\begin{Bmatrix} P_{r1} \\ P_{r2} \end{Bmatrix}$$

where μ_1 and μ_2 are coefficients of friction. Relative velocities at the two junctures are

$$\dot{X}_{r1}=\dot{X}_1-\dot{X}_2, \qquad \dot{X}_{r2}=\dot{X}_3-\dot{X}_4$$

Juncture 1 is assumed sliding with a positive relative velocity, $\dot{X}_{r1}$. Therefore, the pair of physical sliding friction forces which are represented by the symbol P_{f1} are in the direction shown in Fig. 1. These forces are in the positive direction.

Juncture 2 is assumed sticking. The physical sticking attachment forces are assumed in the negative direction, so these forces represented by the symbol P_{st2} are in the direction shown in Fig. 1 for juncture 2.

The P_{ff} and P_{st} matrices are

$$P_{ff}=\begin{Bmatrix} P_{f1} \\ 0 \end{Bmatrix}, \qquad P_{st}=\begin{Bmatrix} 0 \\ -P_{st2} \end{Bmatrix}$$

The P_{ss} matrix from Eq. (3) is

$$P_{ss}=\begin{Bmatrix} P_{f1} \\ -P_{st2} \end{Bmatrix}$$

Juncture 2 remains in the sticking phase as long as $|P_{st2}| < |P_{f2}|$.

Considering Fig. 1, the work done by the force P_{f1} per unit time is

$$-P_{f1}\dot{X}_1+P_{f1}\dot{X}_2=-\dot{X}_{r1}P_{f1} \tag{5}$$

It follows that the modal forces due to the P_{ss} attachment forces are given by

$$P_{qs}=-T_{rs}^T P_{ss} \tag{6}$$

For all discrete dampers, the relative velocities $\dot{d}_r$ are given by

$$\dot{d}_r=T_{rd}\dot{Q} \tag{7}$$

The column matrix of discrete damper forces is given by

$$P_d=T_{nn}D_{nn}+T_nD_n \tag{8}$$

The damper forces from Eq. (8) have the same sign as $\dot{d}_r$. The modal forces due to the discrete dampers are given by

$$P_{qd} = -T_{rd}^T P_d \tag{9}$$

Components of the normal forces at each sliding-sticking juncture are given by

$$P_{io} = T_{ac}\ddot{Q} + T_{df}P_d + T_{fs}P_{ss} + T_{di}Q \tag{10}$$

Load transformation matrices T_{ac}, T_{df}, T_{fs}, and T_{di} are computed by standard structural analysis procedures.

The resultant (squared) matrix of the normal force components at each sliding-sticking juncture are given by

$$P_r^2 = E_1 P_{io}^2 \tag{11}$$

If the P_r^2 matrix is known, P_r is readily computed by always taking the positive square root. This accounts for the sliding friction forces being independent of the direction of the P_r forces.

Initial conditions are static response of the structure due to rigid body acceleration forces and external loads. All sliding-sticking junctures are assumed free to slide for this calculation.

From Eq. (10) it is seen that $\ddot{Q}$ appears implicitly in P_{qs} of Eq. (1). Therefore, an iteration scheme of integration is required.

The ramp and stuck methods differ only in the formulation of the P_{ss} matrix. This matrix is formulated in the Ramp Approach and Stuck Method sections for the two approaches. The numerical procedure is discussed in the Numerical section, while the numerical example is discussed in the Numerical Results section.

Ramp Approach

In the ramp approach, sliding-sticking junctures are always in the sliding phase. Sticking is approximated by taking the coefficient of friction μ as dependent on relative velocity as shown in Fig. 2. Here, $\bar{\mu}$ and $\bar{\dot{X}}_r$ are specified quantities for each sliding juncture. These data permit calculation of the F matrix [see Eq. (2)].

It is seen from Fig. 2 that when the relative velocity is small (less than $\bar{\dot{X}}_r$), the coefficient of friction is less than $\bar{\mu}$. The resulting friction force from Eq. (2), then, is less than a force based on the sliding coefficient of friction. This is the situation during sticking and, therefore, the ramp method gives an approximation to sticking. As there are no sticking attachment forces, the P_{st} matrix is a null matrix and the P_{ss} matrix reference to Eq. (3) is equal to the P_{ff} matrix for the ramp method.

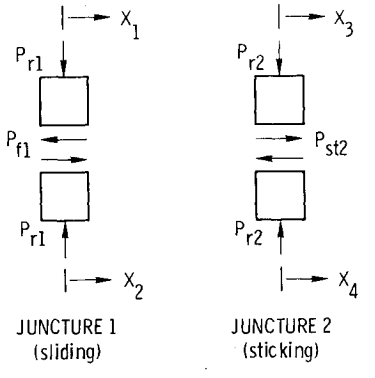

Fig. 1 Attachment forces at sliding and sticking junctures.

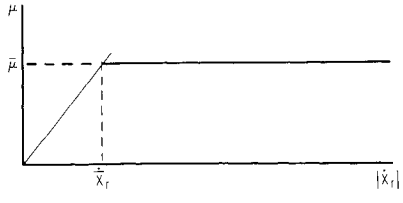

Fig. 2 Coefficient of friction.

Stuck Method

The computer tracks those sliding-sticking junctures which are currently sliding and those which are sticking according to criteria discussed later. Sliding friction forces P_f are computed from Eq. (2) for all sliding-sticking junctures. For the stuck method F is an input matrix. The nonzero values in the P_{ff} matrix are the sliding friction attachment forces for all currently sliding junctures from the P_f matrix but with the same sign as the juncture relative velocity. The nonzero values in the P_{st} matrix are values of attachment forces for all currently sticking junctures. The computation of the P_{st} matrix remains to be explained.

Relative accelerations at the sliding-sticking junctures are considered, and these are given by

$$\ddot{X}_r = T_{rs}\ddot{Q} \tag{12}$$

The equation of motion, Eq. (1), is written as

$$\ddot{Q} = X + P_{qs} \tag{13}$$

From Eqs. (12) and (13), relative accelerations at all sliding-sticking junctures are given by

$$\ddot{X}_r = T_{rs}X + T_{rs}P_{qs} \tag{14}$$

When the relationship given by Eq. (3) is substituted into Eq. (6), the result is

$$P_{qs} = -T_{rs}^T\{P_{ff} + P_{st}\} \tag{15}$$

When Eq. (15) is substituted into Eq. (14), the result is

$$\ddot{X}_r = T_{rs}X - T_{rs}T_{rs}^T P_{ff} - T_{rs}T_{rs}^T P_{st} \tag{16}$$

Attachment forces at sticking junctures are the only nonzero values in the P_{st} matrix. Consider now how these P_{st} values are obtained from Eq. (16).

The relative accelerations of all sticking junctures are set to zero in the $\ddot{X}_r$ matrix on the left-hand side of Eq. (16). On the right-hand side of the equation both matrices X and P_{ff} are known. Recall that P_{ff} is a matrix of sliding friction forces with zero values corresponding to all sticking junctures. The latest updated information is used to form the P_{ff} matrix.

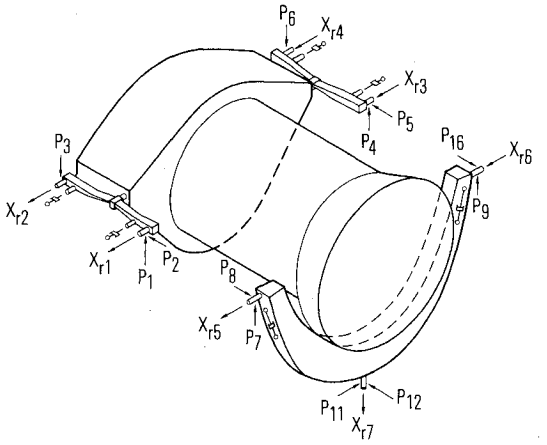

Fig. 3 Payload, normal force components, and sliding displacements.

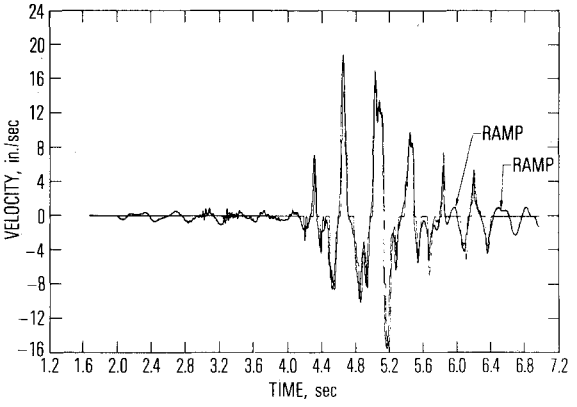

Fig. 4 Relative velocity ramp and stuck.

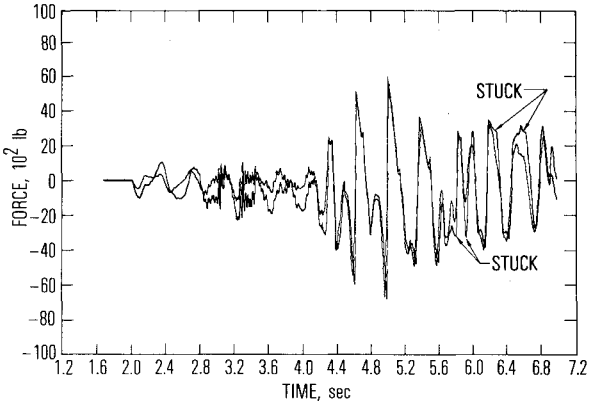

Fig. 5 Attachment force ramp and stuck.

Then Eq. (16) will account for all of the attachment force discontinuities which are described shortly.

The unknowns in Eq. (16) are the attachment forces at all stuck junctures and the relative accelerations at all sliding junctures. From Eq. (16), the number of linear equations equals the number of unknowns so all unknowns can be determined.

When the relative velocity at a sliding juncture changes sign, it is possible that the juncture is sticking. If an initial sticking attachment force exceeds the magnitude of the corresponding sliding friction force magnitude in the P_f matrix, the sliding juncture has a relative velocity sign change without sticking. Otherwise, the juncture is in the sticking phase. A juncture goes from the sticking phase to the sliding phase when its attachment force value in the P_{st} matrix exceeds in magnitude the corresponding value of the sliding friction force in the P_f matrix.

In the case where the relative velocity of a sliding juncture changes sign without sticking, the sliding friction force changes direction suddenly so there is a discontinuity in the attachment force. In general, when a juncture goes from the sliding phase to the sticking phase, the sliding friction force just before sticking does not equal the sticking force just after sticking, so there is a discontinuity in this attachment force. Note that discontinuities in attachment forces result in discontinuities in modal acceleration, $\ddot{Q}$.

Numerical Procedure

The equations of motion are solved numerically by first converting Eq. (1) to a system of first-order differential equations and then using a Runge-Kutta-Adams-Moulton integration procedure.[4] Given Q and $\dot{Q}$ at time t, $\ddot{Q}$ is determined at time t, and Q and $\dot{Q}$ at time $t+\Delta t$.

This is complicated by the fact that $\ddot{Q}$ appears implicitly in the term P_{qs}. This dependence appears in Eq. (10). The P_{ss} matrix [see Eq. (6)] depends on itself as it also appears in Eq. (10). Therefore, $\ddot{Q}$ and P_{ss} are determined iteratively, starting with their values from the previous time step.

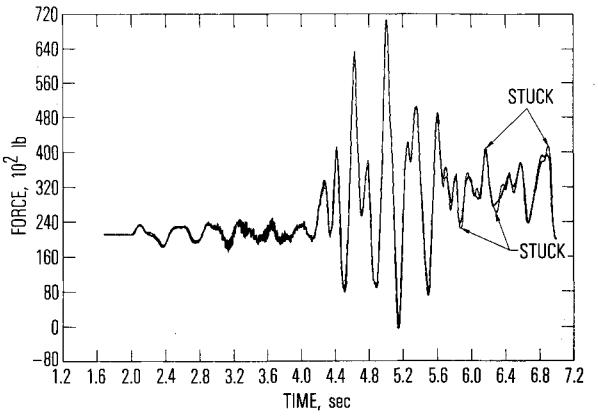

Fig. 6 Normal force component ramp and stuck.

Three iterations on $\ddot{Q}$ and P_{ss} were required in the ramp method. Two iterations were sufficient for the stuck method. This partially offsets the increased computer time for the stuck method but still leaves a computer time ratio of 3/2 favoring the ramp method over the stuck method.

The Runge-Kutta portion of the algorithm is used during the first few steps until enough values are on hand for the Adams-Moulton portion to be used. For the stuck method, the Runge-Kutta portion was also used each time a juncture altered from sliding to sticking or sticking to sliding because of the discontinuities present during the transaction.

Numerical Results

The inertial upper stage payload is shown in Fig. 3. Normal force components and sliding displacements relative to the Space Shuttle are noted. The payload merged with the Space Shuttle had a total of 347 modes. For the nonlinear dynamic response, the first 225 modes were retained. Modal damping of 1% was assumed.

Numerical results were obtained for the ramp and stuck methods, considering a liftoff loading condition. Coefficient of friction assumed for the stuck method was $\mu = 0.10$ and $\bar{\mu} = 0.10$, $\bar{X}_r = 2.0$ in./s (see Fig. 2) for the ramp method.

Plotted response data as standard computer output included components of normal forces P_{io}, relative sliding displacements and velocities X_r and $\dot{X}_r$, and attachment forces at sticking and sliding junctures P_{ss}.

For the ramp and stuck methods, relative velocity and the attachment force corresponding to X_{r1} are shown in Figs. 4 and 5. A comparison of the normal force component P_2 is shown in Fig. 6. These comparisons illustrate the good agreement between the results of the ramp and stuck methods.

Results also were obtained without friction. A comparison of the normal force component P_2 and relative displacement X_{r1} with and without friction, shown in Figs. 7 and 8, gives a measure of the friction effect.

Sine-dwell computer runs using the stuck method were made of the payload shown in Fig. 3, supported by a rigid fixture, so as to simulate a modal test. The payload was represented by 20 modes, assuming 1% modal damping and $\mu = 0.10$. Computer runs were made with one modal force nonzero, the other 19 zero, and no dead weight loading.

The result indicated that modes are always excited in addition to the mode corresponding to the nonzero modal force. These other modes have modal accelerations as much as 1/10 the acceleration of the resonant mode, and their excitation can be at a higher frequency than the modal force.

This excitation impacts the feasibility of modal testing of structures with sliding junctures. It is due to the sliding friction forces.

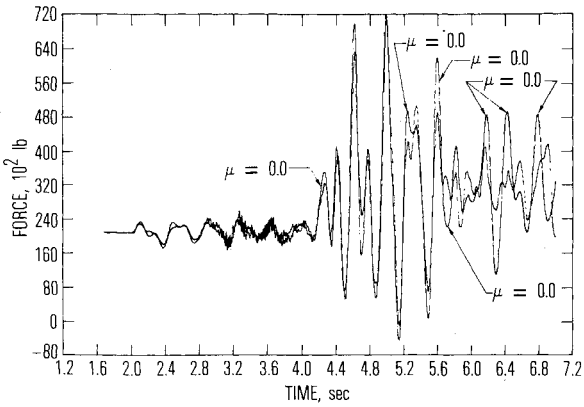

Fig. 7 Normal force component with and without friction.

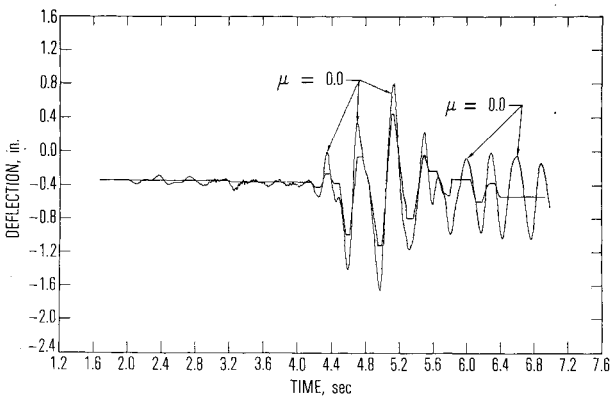

Fig. 8 Relative displacements with and without friction.

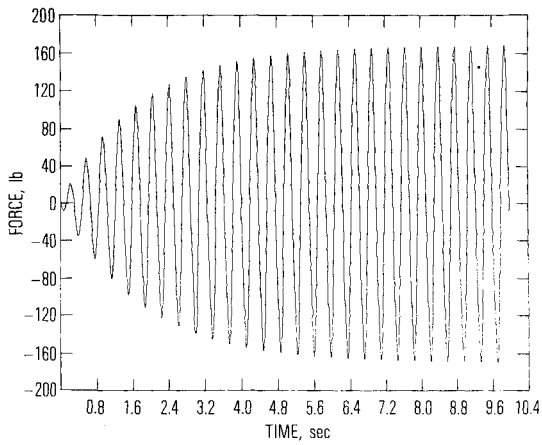

Fig. 9 Component of normal force sine-dwell.

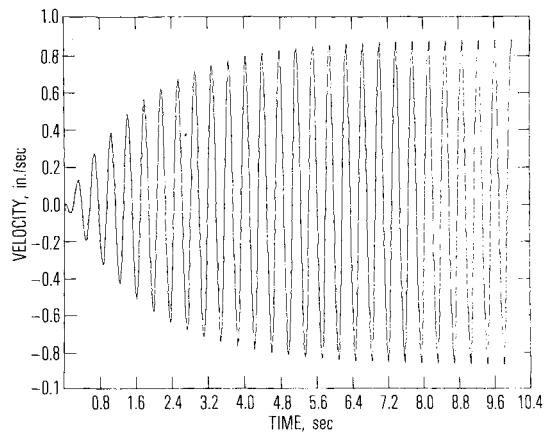

Fig. 10 Relative sliding velocity sine-dwell.

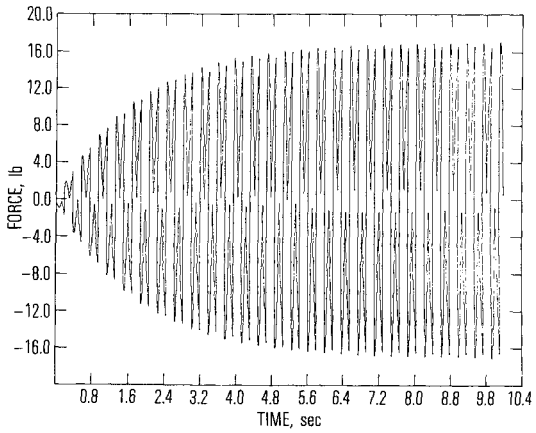

Fig. 11 Attachment force sine-dwell.

Both the normal forces and relative sliding velocities are at the modal force frequency. The magnitude of the sliding friction force is μ times the normal force. Its direction depends on the sign of the relative velocity. Due to the phase angle between normal force and relative velocity, there are additional oscillations in the sliding friction and sticking attachment forces. This phenomenon is illustrated by typical computer results shown in Figs. 9-11.

Conclusions

The good comparison of the results of the ramp and stuck methods gives a check of the formulation and coding. The comparison of relative velocity from the ramp and stuck methods illustrates a smoothing-out effect on velocity from the ramp method during sticking. The results considering attachment forces and relative velocity show that the ramp method simulates sticking fairly well when $\dot{X}_r$ (Fig. 2) is less than 1/10 of the maximum juncture relative velocity.

For sine-dwell excitation, the results from the stuck method indicate that discontinuities in accelerations are important. Therefore, the stuck method more closely simulates the nonlinear response of structures with sliding friction junctures, especially during sine-dwell excitation, than the ramp method.

Acknowledgments

The authors wish to acknowledge H. A. Bagwell and R. F. Kramer of The Aerospace Corporation for their suggestions concerning numerical procedures. T. B. Jones of The Aerospace Corporation was responsible for obtaining program office support and assisted with code formulation. The plotting portion of the computer program was coded by H. A. Bagwell.

This study was supported by the Space Division, Air Force Systems Command, under Contract F04701-81-C-0082.

References

[1] Hunt, D. A., "Dynamic Analysis of a Flexible Vehicle Moving Along a Flexible Support," *Journal of Spacecraft and Rockets*, Vol. 8, June 1971, pp. 665-668.

[2] Timoshenko, S. P., *History of Strength of Materials*, McGraw-Hill Book Co., New York, 1953, pp. 173-178.

[3] MacNeal, H. R., ed., *The Nastran Theoretical Manual*, (Level 15.0), NASA SP-221(01), Dec. 1972, p. 11.2-3.

[4] Lapidus, L. and Seinfeld, J. H., *Numerical Solution of Ordinary Differential Equations*, Academic Press, New York, 1971, pp. 41-43, pp. 180-183.